*Int. J. Electrochem. Sci.*, 10 **(2015)** 432 - 444

International Journal of
ELECTROCHEMICAL
SCIENCE
www.electrochemsci.org

# Microscopy and Electroanalysis of a First Generation Copper-poly(propyleneimine) Metallodendrimer System

*Candice Rassie*[*], *Juanita van Wyk*[1], *Lindsay Wilson, Hlamulo R. Makelane, Usisipho Feleni, Unathi Sidwaba, Selwyn Mapolie*[2], *Priscilla Baker, Emmanuel Iwuoha*

Department of Chemistry, University of the Western Cape, Bellville, 7535, Cape Town, South Africa
[1] Currently at Department of Chemistry, University of the Witwatersrand, Johannesburg, South Africa.
[2] Currently at Department of Chemistry, Stellenbosch University, Stellenbosch, South Africa.
[*]E-mail: 2734778@myuwc.ac.za and eiwuoha@uwc.ac.za

*Received:* 13 October 2014 / *Accepted:* 24 November 2014 / *Published:* 2 December 2014

A copper-poly(propyleneimine) (CuPPI) metallodendrimer was physically adsorbed onto the surface of a gold electrode to form an Au|CuPPI electrode system, which was electrochemically characterized by cyclic and square wave voltammetric techniques. The CuPPI metallodendrimer was found to be electroactive on Au electrode and has diffusion coefficient (*D*) values of 4.124 x $10^{-5}$ $cm^2$ $s^{-1}$ (in the absence) and 3.29 x $10^{-5}$ $cm^2$ $s^{-1}$ (in the presence) of oxygen in the cell solution. The surface morphology of the poly(propyleneimine) dendrimer (PPI) and its copper-functionalized derivative, i.e. CuPPI, were compared using atomic force microscopy (AFM). High resolution transmission electron microscopy (HR-TEM) and high resolution scanning electron microscopy (HR-SEM) data showed that CuPPI has a layered crystalline structure. The metallodendrimer would be a suitable platform for electrochemical biosensing applications since the diffusion coefficient is only very slightly affected by oxygen.

**Keywords:** Metallodendrimer, copper, HR-TEM, HR-SEM, electrochemical characterization.

## 1. INTRODUCTION

Dendrimers are synthetic molecules which have a roughly spherical and highly branched structure and can also be described as dendritic polymers, since they consist of a number of monomer units which are chemically linked together [1]. The spherical and 3-dimensional structure of the dendrimer gives it ideal conductive characteristics to be used as an electrocatalytic membrane that assists in the transport of electrons i.e. ideal conducting platform. Dendrimers have attracted interest because of their ability not only to perform as a host/guest but also their ability to be functionalized in

the core as well as on the periphery [2]. Dendrimers built around a metal core can be described as metal complexes of ligands carrying dendritic substituents [3]. The shape, size and catalytic activity of the metallodendrimer is directly dependant on the type of metal incorporated as well as the location of said metal. Lower generation dendrimers such as 1 or 2 were found to be more useful in catalysis due to their open and symmetric structures which allow for fast electron transfers [4]. These molecules are considered versatile because of ease of modifications and have thus found various applications including drug delivery [1] [5], gene delivery [6], magnetic resonance imaging contrast agents [7] and for our purpose sensors [8] [9]. Dendrimers have also been used as macromolecule supports in catalysis [10] as models for self-assembled monolayers [11] and even as chemiresistors [12]. The unique structure of the dendrimer can help with selectivity of sensors by only allowing certain molecules to reach its target [8] [13]. It can also be used as an electrocatalytic platform for DNA biosensing as previously reported [14]. Electrochemical sensors have been proven to be the most viable candidate recently for their many advantages compared to other types of sensors. These include the potential for real time monitoring, low cost and point of care diagnostics. Electrochemical technology is simplistic, sensitive as well as specific which makes it applicable to a wide variety of sensor applications [15]. Previous studies of first generation copper, cobalt and nickel poly(propyleneimine) metallodendrimers have been carried out and found to be electroactive and a viable candidate for biosensing purposes as well [16]. In this work a copper based metallodendrimer will be characterized to determine its structural properties using high resolution microscopy as well as its electrochemical properties using voltammetric techniques. The copper poly(propyleneimine) based dendrimer was physically adsorbed onto the surface of a gold working electrode before electrochemical characterization to be used as a future platform for electrochemical biosensing.

## 2. EXPERIMENTAL SECTION

### *2.1. Materials and Methods*

Sodium dihydrogen phosphate ($NaH_2PO_4$), disodium hydrogen phosphate ($Na_2HPO_4$), sodium chloride (NaCl), sulfuric acid ($H_2SO_4$), hydrogen peroxide ($H_2O_2$), ethanol and acetone were purchased from Sigma Aldrich and used as received. Ultra-pure water was used in all aqueous solutions and throughout the experiment, purified by a Milli-$Q_{TM}$ system (Millipore). The dendrimer and metallodendrimer were synthesized using a similar method as shown in [17]. In this case a functionalized benzene group was used in the place of the pyrrole-2-carboxylaldehyde during synthesis of the ligand/dendrimer as well as the metallodendrimer used in this work.

### *2.2. Instruments*

The electrochemical experiments were carried out in a three electrode system consisting of working, counter and reference electrodes in a 10 ml glass cell. The working electrode was gold with a diameter of 1.6 mm. The reference electrode was Ag/AgCl (3 M $Cl^-$) and platinum wire served as the

counter electrode. All electrodes were obtained from BASi. Analytical grade argon (Afrox, South Africa) was used for purging the system in anaerobic experiments. Alumina polishing pads and powder (0.05, 0.3 and 1.0 μm) were obtained from Buehler, Illinois, USA. All cyclic voltammetry and square wave voltammetry experiments were carried out on BASi epsilon. Infrared spectrum of the dendrimer and its copper functionalized metallodendrimer was obtained using PerklinElmer Spectrum 100-FT-IR Spectrometer. High resolution transmission electron microscopic (HR-TEM) images of the dendrimer and its copper functionalized metallodendrimer were obtained using a Tecnai G2 F2O X-Twin MAT microscope. The characterization of the compounds via HR-TEM was carried out by placing a drop of the dendrimer/metallodendrimer solution onto a carbon coated nickel grid which was allowed to dry for a day before analysis. High resolution scanning electron microscopy (HR-SEM) was carried out on the materials using a Zeiss Auriga HR- SEM. Atomic force microscopy (AFM) imaging was carried out on a Veeco NanoMan V model.

### *2.3. Electrochemical Characterization*

The working electrode was cleaned before each experiment by polishing to a mirror like surface on polishing pads with alumina powder of 1, 0.3 and 0.05 micron respectively. This process was the followed by sonication of the electrode in ethanol and water for 5 and 10 min respectively. Electrochemical cleaning of the electrode was also carried out by cycling in a 1 M solution of sulfuric acid. Ten cycles were done between the potentials of -200 mV and 1500 mV or until a reproducible voltammogram was obtained. A 5 mM solution of dendrimer (PPI or CuPPI) was prepared using 1:1 (v/v) acetone-ethanol. A volume of 8 μL of the dendrimer solution was then drop-coated onto the surface of the clean gold electrode and left to dry for 45 min to allow for physical adsorption to take place. The surface of the electrode was then rinsed lightly with ethanol to remove any unbound dendrimer and dried under a stream of nitrogen gas. The resulting electrode will be called Au|PPI or Au|CuPPI. The electrodes were characterized in 0.1 M phosphate buffer pH 7.4 within a window potential of -600 mV to 600 mV using cyclic voltammetry and square wave voltammetry (frequency of 10 Hz and amplitude of 25 mV).

## 3. RESULTS AND DISCUSSION

### *3.1. Characterization of dendrimer and metallodendrimer*

The copper metallodendrimer was first characterized using imaging techniques such as HR-TEM, HR-SEM and AFM in order to compare the differences in surface morphology as well as structure between the dendrimer and its copper functionalized counterpart. The structures of the two different dendrimers are as shown in Figure 1.

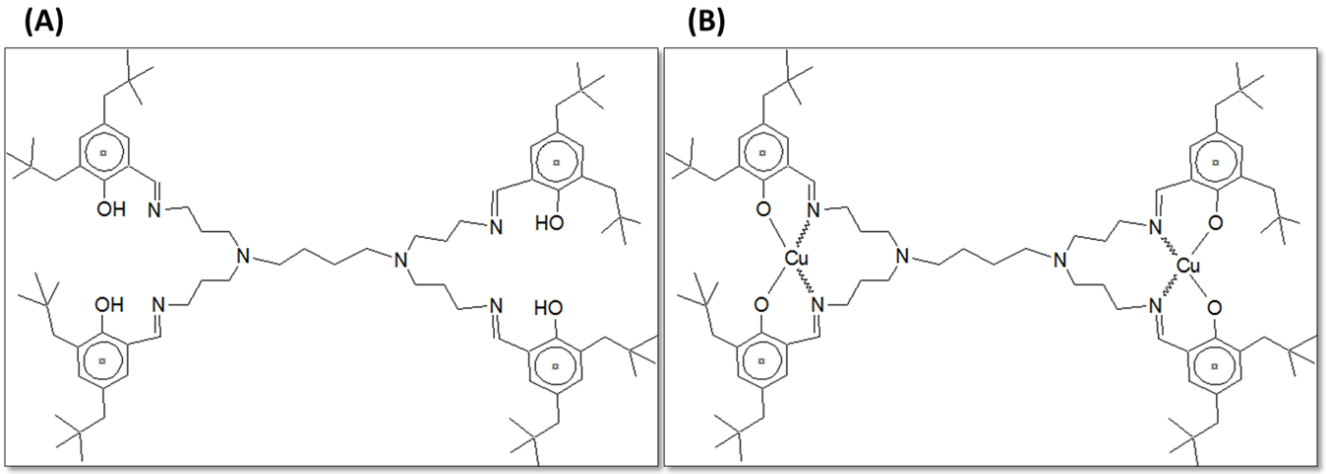


**Figure 1**. Dendrimers (A) polypropyleneimine dendrimer/PPI (B) copper polypropyleneimine metallodendrimer/CuPPI

In order to confirm the presence of copper within the CuPPI system the two samples were investigated using Fourier transform infrared spectroscopy (FTIR). The copper element was incorporated into the PPI dendrimer in order to enhance the electrocatalytic capabilities of the compound. The CuPPI spectrum shows a *ν*(C–N) stretching band at 1084 $cm^{-1}$ and a *ν*(N–H) bending band at 1527 $cm^{-1}$ [14]. These are absent or less pronounced in the FTIR spectra of PPI. The shift in the ν(C=N) stretching band at 1632 $cm^{-1}$ in PPI to 1628 $cm^{-1}$ in CuPPI as well as the appearance of a new band at 1527 $cm^{-1}$ in the spectrum of the CuPPI complex strongly suggests nitrogen–copper coordination [18]. The new band at 525 $cm^{-1}$ could be attributed to copper (Cu–O) band in the spectrum of CuPPI [19].

The AFM and HR-TEM images of the PPI dendrimer show a rather smooth surface morphology with no distinct features. Dendrimers have a roughly spherical structure which could be the reason for the aggregates as shown in the AFM and HR-TEM images below. We then went on to study the PPI dendrimer using HR-SEM imaging at a magnification of 5 KX as well as 50 00 KX. These images compliment the other imaging techniques in the sense that the dendrimer does not have an ordered or crystalline structure as shown in Figure 2.

Studies were carried out using these same techniques on the copper functionalized metallodendrimer i.e. CuPPI. These results are as shown in Figure 3. All imaging techniques used show a vast difference in the surface morphology as well as the structure of the metallodendrimer compared to the dendrimer, which does not have copper incorporated into its structure. The AFM results show a more rugged and rough surface morphology compared to the PPI dendrimer. The HR-TEM images reveal that the presence of copper caused the dendrimer to become crystalline as shown by the lattice fringes in Figure 3(B). The experimental lattice fringe spacing is consistent with the interplanar spacing of the [111] plane of the CuPPI dendrimer [20]. HR-SEM results further confirm the ordered nature of a crystalline substance that allows the metallodendrimer to form sheets of CuPPI instead of clumps as with the PPI dendrimer.

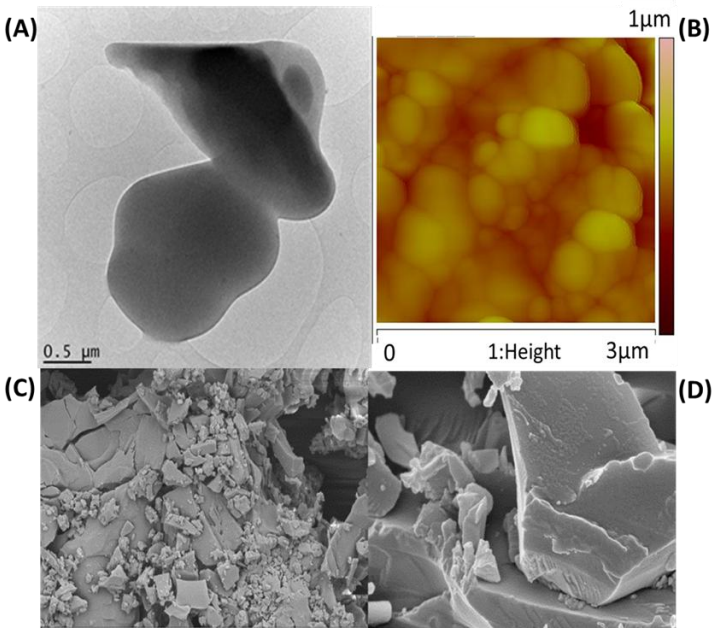


**Figure 2**. Surface morphology studies of PPI: (A) HR-TEM (B) AFM (C) and (D) HR-SEM

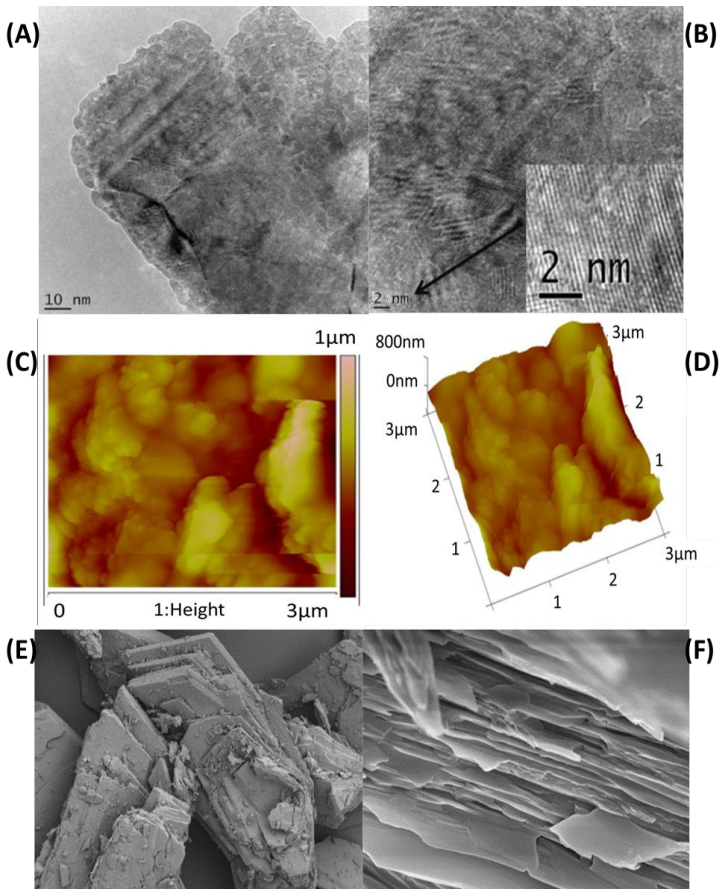


**Figure 3**. Surface morphology studies of CuPPI: (A) and (B) HR-TEM (C) and (D) AFM (E) HR-SEM at 505 X (F) HR-SEM at 50 00 KX

The fact that the CuPPI is more ordered and forms self-assembled layers well, as well as the fact that it is theoretically more conductive than PPI makes it a more favorable candidate for an application in an electrochemical sensor.

### *3.2 Electrochemical characterization of Au|PPI*

In order to verify the advantages of the CuPPI metallodendrimer over the PPI dendrimer, the two compounds were characterized using electrochemical techniques such as cyclic voltammetry and square wave voltammetry. The results of the PPI dendrimer electrochemical characterization are as shown in Figure 4.

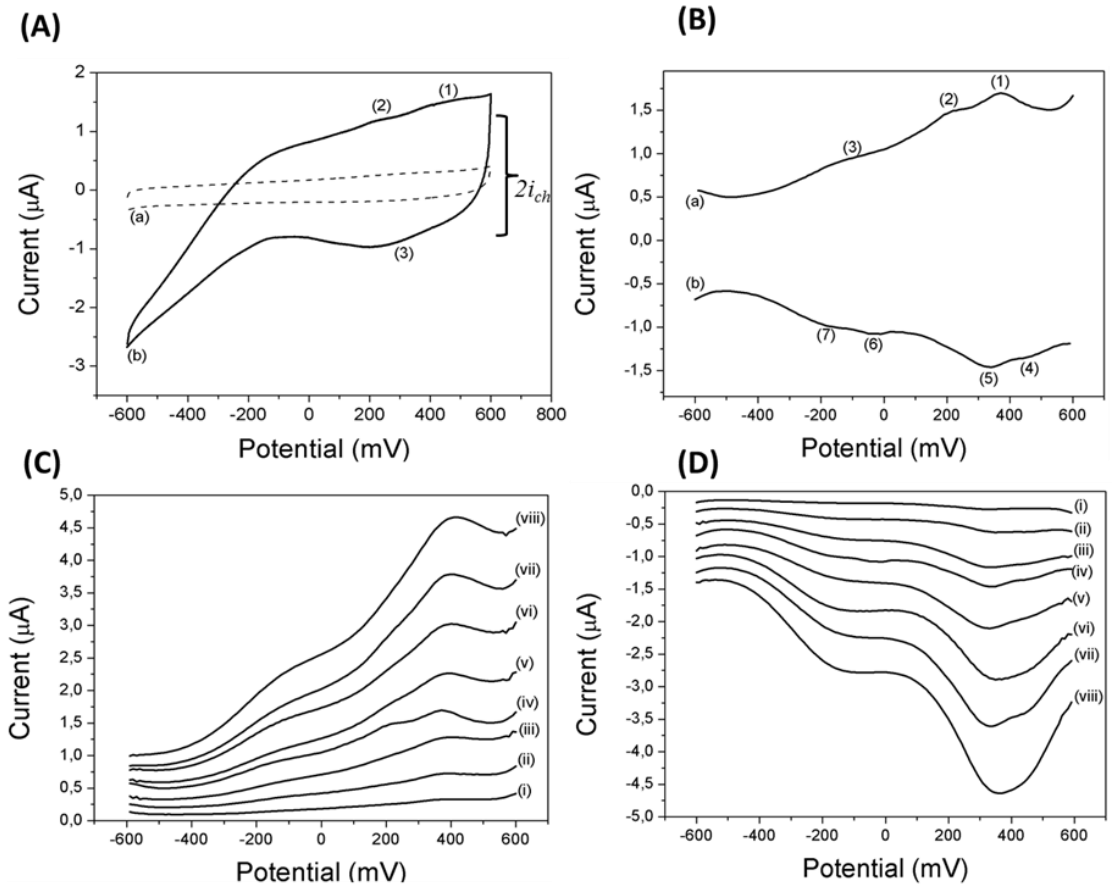


**Figure 4**. (A) cyclic voltammograms of (a) bare gold electrode (b) PPI coated electrode at 100 mV/s (B) square wave voltammograms of (a) anodic and (b) cathodic scans of PPI coated gold electrode at 10 Hz (C) anodic square wave voltammograms of PPI coated gold electrode at frequencies of (i) 2 (ii) 5 (iii) 8 (iv) 10 (v) 15 (vi) 20 (vii) 25 and (viii) 30 Hz (D) cathodic square wave voltammograms of PPI coated gold electrode at above frequencies.

The cyclic voltammogram of PPI shows some electroactivity, much more than the bare gold electrode on which it was deposited. Although no distinct peaks are shown in the CV shown in Figure

4 (A), there are "shoulders" visible at around 400 mV (1) and 200 mV (2) in the anodic scan ($E_{pa}$) and 320 mV (3) in the cathodic scan ($E_{pc}$); these could be viewed better using the more sensitive technique of SWV. In the square wave voltammogram in Figure 4 (B) anodic scan peaks were present at $E_{pa}$ = 370 mV (1), 200 mV (2) and a shoulder at -130 mV (3). Four peaks were observed in the cathodic scan ($E_{pc}$) of the SWV at $E_{pc}$ = 480 mV (4), 335 mV (5) and two smaller ones at -40 mV (6) and -190 mV (7). These are due to the oxidation of the four hydroxyl groups within the structure of the PPI dendrimer which occur in a complex cascade reaction and their subsequent reduction in the cathodic scan [16]. One can notice that the charging current ($i_{ch}$) of the PPI dendrimer is quite large in this case in comparison with the faradaic current (current generated from reduction or oxidation at electrode surface). The charging current is also known as the capacitive current and does not involve any chemical reactions at the electrode surface. It only causes accumulation or removal of electric charges on the electrode and in the electrolyte surface near the electrode. Since in this case the charging current is quite large in the cathodic sweep, one can deduce that the oxidized form of the dendrimer has a high resistance.

To determine the reversibility of the system one can refer to Nernst Equation 1.

$$\Delta E = \left| E_{pa} - E_{pc} \right| = \frac{2.3030\,RT}{nF} \quad \text{.....Equation 1 [21]}$$

Where $E_{pa}$ and $E_{pc}$ are the anodic and cathodic peak potentials respectively, $R$ is the gas constant 8,314 J $K^{-1}$ $mol^{-1}$, $n$ is the number of electrons transferred and $F$ is Faradays constant 96485 C $mol^{-1}$. The number of electrons involved in the electrochemical process can be estimated from equation above. Therefore, for a reversible redox reaction at 25 °C (298 K) with $n$ electrons $\Delta E$ should be 0.0592/n V or about 60 mV for one electron. Since the peak separation in the case of the PPI dendrimer is 80 mV we can deduce that the number of electrons transferred is 1 and the reaction is quasi-reversible because 0.0592/n V is more than 60 mV. The PPI dendrimer was then characterized at various frequencies in order to determine the diffusion processes in the system. It can be seen that at higher frequencies the shoulder peaks present at negative potentials become more prominent. This can be due to fast electron processes or transfers within the dendrimer system. There is a good linear relationship between peak current and frequency in the SWV with a correlation coefficient of 0.90 and 0.89 for the anodic and cathodic peak currents respectively according to Equation 2.

$$\Delta i_p = 0.665nFAC_o^* \frac{D_o^{1/2}}{\pi^{1/2}} f^{1/2} \text{.....Equation 2 [22]}$$

*3.3 Electrochemical characterization of Au|CuPPI*

The CuPPI metallodendrimer was then characterized using cyclic voltammetry as shown in Figure 5. In comparison, the CuPPI dendrimer has much more electrocatalytic behavior compared to the PPI dendrimer. More pronounced peaks are seen as well as a reversible one electron transfer process in the CuPPI dendrimer according to Equation 1 [21]. Two major peaks appear in the cyclic voltammogram in Figure 5 (A) at $E_{pa}$ = 220 mV (1) and $E_{pc}$ = 180 mV (2) resulting in a peak separation of $\Delta E$ = 40 mV. These two major peaks can be attributed to the oxidation of Cu(I) at a negative potential to its normal state of Cu(II) during the anodic scan and the subsequent reduction back to Cu(I) during the cathodic scan. The peaks previously attributed to the PPI ligand are still

visible as shoulders in the cyclic voltammogram of the metallodendrimer as peaks 3, 4 and 5. The anodic peaks attributed to the PPI ligand at 370 mV have now shifted to 400 mV (3) and the cathodic peak originally at 335 mV is still present as a small shoulder around 360 mV (4). The other cathodic peak previously present at -40 mV is now more visible at -100 mV (5). Once again the charging current for the cathodic sweep is quite large, again indicating that the oxidized form of the dendrimer has a high resistance and thus requires a greater flow of electrons in order to reduce the compound.

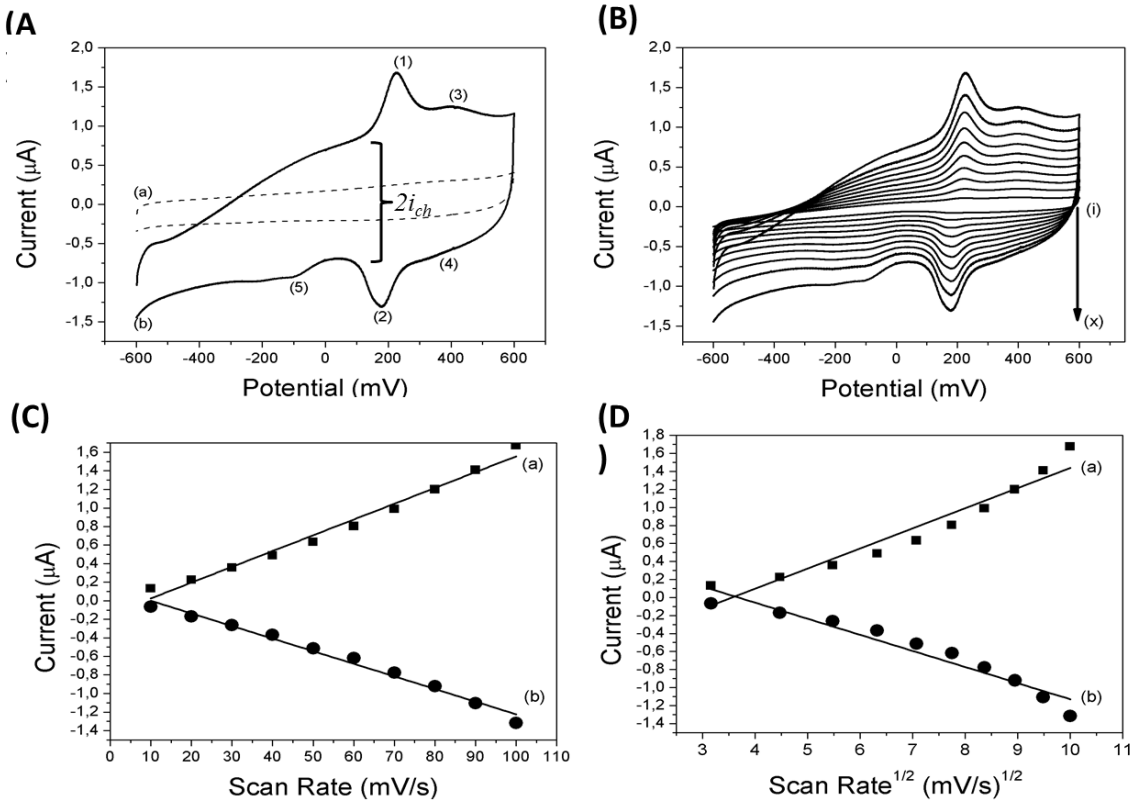


**Figure 5**. (A) cyclic voltammograms of (a) bare gold electrode and (b) CuPPI coated gold electrode at 100 mV/s (B) cyclic voltammograms of CuPPI coated gold electrode at scan rates of (i) 10 to (x) 100 mV/s at 10 mV/s intervals (C) linear plot of current vs scan rate (D) linear plot of current vs square root of scan rate.

The CuPPI dendrimer was also run at varying scan rates and shows a good linear relationship and correlation coefficient of 0.96 between current and scan rate as shown in Figure 5 (B) and (C). The anodic non shifting peak will now be analyzed in order to determine the surface concentration as well as diffusion coefficient of the electrocatalytic system according to the Brown Anson Equation 3 where the surface area of the electrode is A = 0.0201 cm$^2$. In this case the plot of current vs scan rate will be used.

$$I_p = \frac{n^2 F^2}{4RT} \nu A \Gamma_O$$ .....Equation 3 [23]

The surface concentration of the electrocatalytic platform of metallodendrimer was found to be $\Gamma_O$ = 9.014x10$^{-7}$ mol cm$^{-2}$. This shows that a generous amount of dendrimer was immobilized on the

surface and that physical adsorption of dendrimer was successful. The diffusion coefficient was also calculated using the Randles Sevcik Equation 4 where $C_0$ = 0.1 M, $n$ is assumed to be 1 and the surface area of the electrode is the same. In this case the plot of current vs square root of scan rate will be used as shown in Figure 5 (D).

$$I_p = 2.69x10^5\, n^{3/2} A D^{1/2} v^{1/2} C_O$$ ……..Equation 4 [24]

The diffusion coefficient of this CuPPI metallodendrimer system was calculated to be $D$ = 4.124x10$^{-5}$ cm$^2$ s$^{-1}$. A square wave voltammetry experiment of the CuPPI metallodendrimer was also carried out in order to verify the results obtained in the CV experiment. The SWV experiment as shown in Figure 6 (A) produced a major anodic peak at 216 mV (1) with another smaller peak at 380 mV (2) with a shoulder at -40 mV (3).

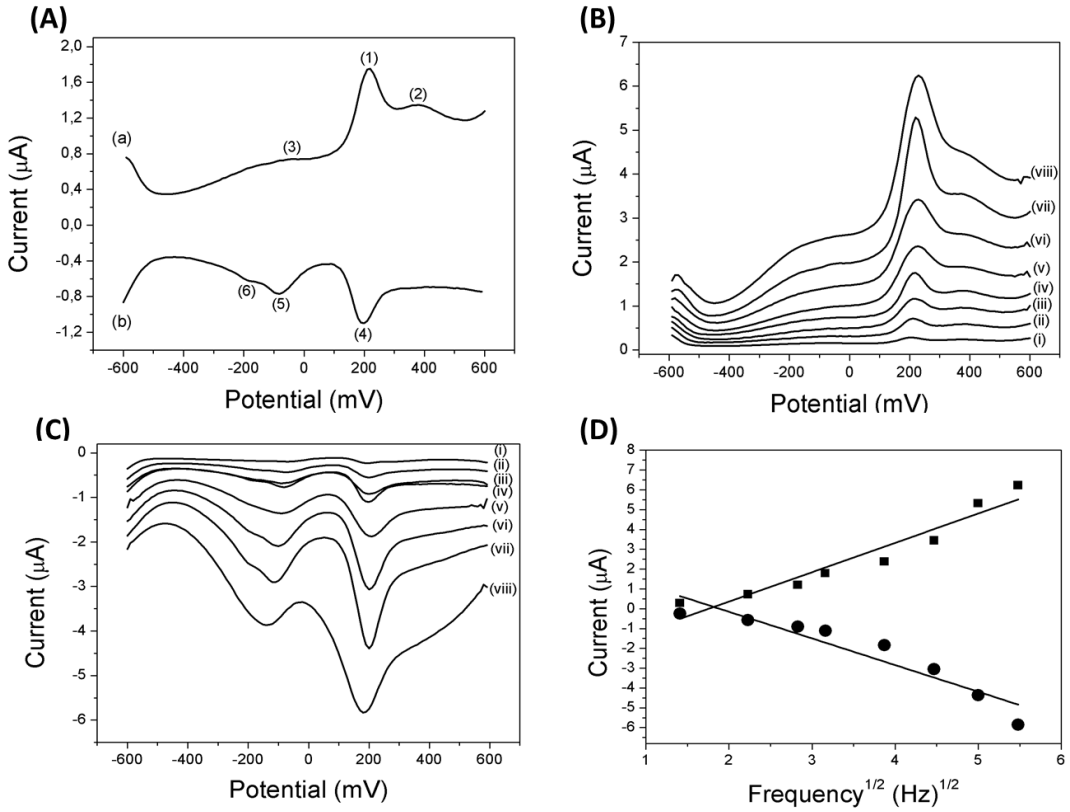


**Figure 6**. (A) square wave voltammograms of (a) anodic and (b) cathodic scans of CuPPI coated gold electrode at 10 Hz (B) anodic square wave voltammogram of PPI coated gold electrode at frequencies of (i) 2 (ii) 5 (iii) 8 (iv) 10 (v) 15 (vi) 20 (vii) 25 and (viii) 30 Hz (C) cathodic square wave voltammograms of PPI coated gold electrode at above frequencies (D) linear plot of current vs frequency.

The cathodic scan produced a major peak at 200 mV (4) with a smaller one at -80 mV (5) with a shoulder present at -180 mV (6). Again in this case it is clear that a complex cascade oxidation of the hydroxyl groups are taking place in the metallodendrimer with the major peaks being attributed to the oxidation of Cu(I) to Cu(II) and its subsequent reduction [16]. The CuPPI metallodendrimer was also

run at various frequencies and the peaks in the negative region was amplified at higher frequencies as before with the PPI dendrimer as shown in Figure 6 (B) and (C). These results show that the CuPPI platform has a good linear relationship between peak current and the frequency at which the scan is carried out according to Equation 2 [22]. In this case a correlation coefficient of 0.90 and 0.87 were obtained for the anodic and cathodic peaks respectively as illustrated in Figure 6 (D).

### *3.4. The effect of oxygen on the Au|CuPPI system*

We then went on to test the effect of oxygen in the Au|CuPPI system using cyclic voltammetry. This was done in order to determine not only the interference of oxygen in the system but also as one step in testing whether a future biosensor would be applicable to real samples using this compound as a platform. A cathodic peak ($E_{pc}$) appeared at around -400 mV with and without CuPPI on the gold working electrode was noted. We can thus attribute these peaks to the reduction of oxygen within the system. The Au|CuPPI was also run at varying scan rates in the presence of oxygen in order to determine the diffusion coefficient using Equation 4 as previously shown and was found to be $D$ = $3.29 \times 10^{-5}$ $cm^2$ $s^{-1}$. Since the diffusion coefficient is slightly lower in the presence of oxygen we can assume that the oxygen has some kind of interfering effect on electronic processes happening on the surface of the electrode, but not much.

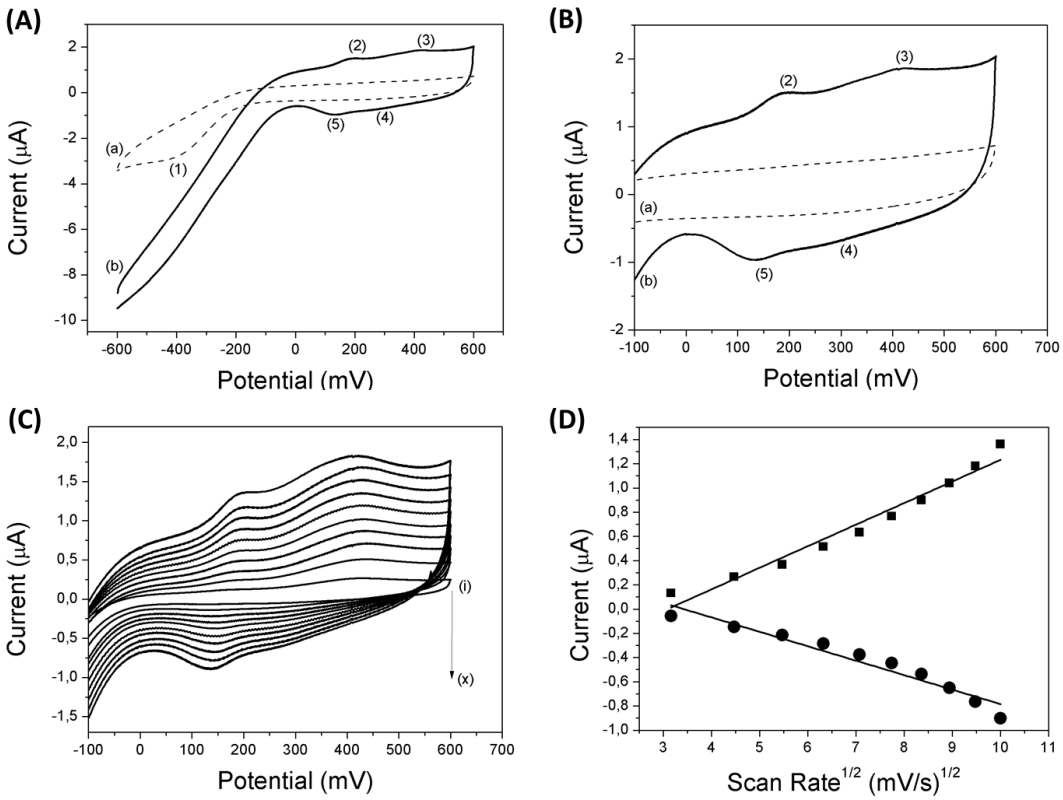


**Figure 7**. (A) cyclic voltammograms of (a) bare gold electrode and (b) CuPPI coated gold electrode at 100 mV/s (B) enlargement of A (C) cyclic voltammograms of CuPPI coated gold electrode at scan rates of (i) 10 mV/s to (x) 100 mV/s at 10 mV/s intervals (D) linear plot of current vs square root of scan rate. All of the above were carried out under aerobic conditions.

Square wave voltammetry was also carried out on Au|CuPPI in aerobic conditions. The anodic scan resulted in three peaks at $E_{pa}$ = -200 mV, 182 mV and 388 mV. The cathodic scan resulted in two peaks at $E_{pc}$ = -186 mV and 170 mV. The anodic peak at 388 mV is thus attributed to the oxygen present in the system as well as the cathodic peak at -186 mV. The peaks at 170 mV and 182 mV are therefore confirmed to be characteristic of the CuPPI dendrimer. When increasing the frequency within square wave it was found that the peaks originating from the reduction of oxygen increase in intensity. This might be indicative of fast electron processes at the electron surface. Again the peak current has good correlation with frequency in this case 0.93 and 0.93 for anodic and cathodic peaks respectively according to Equation 2.

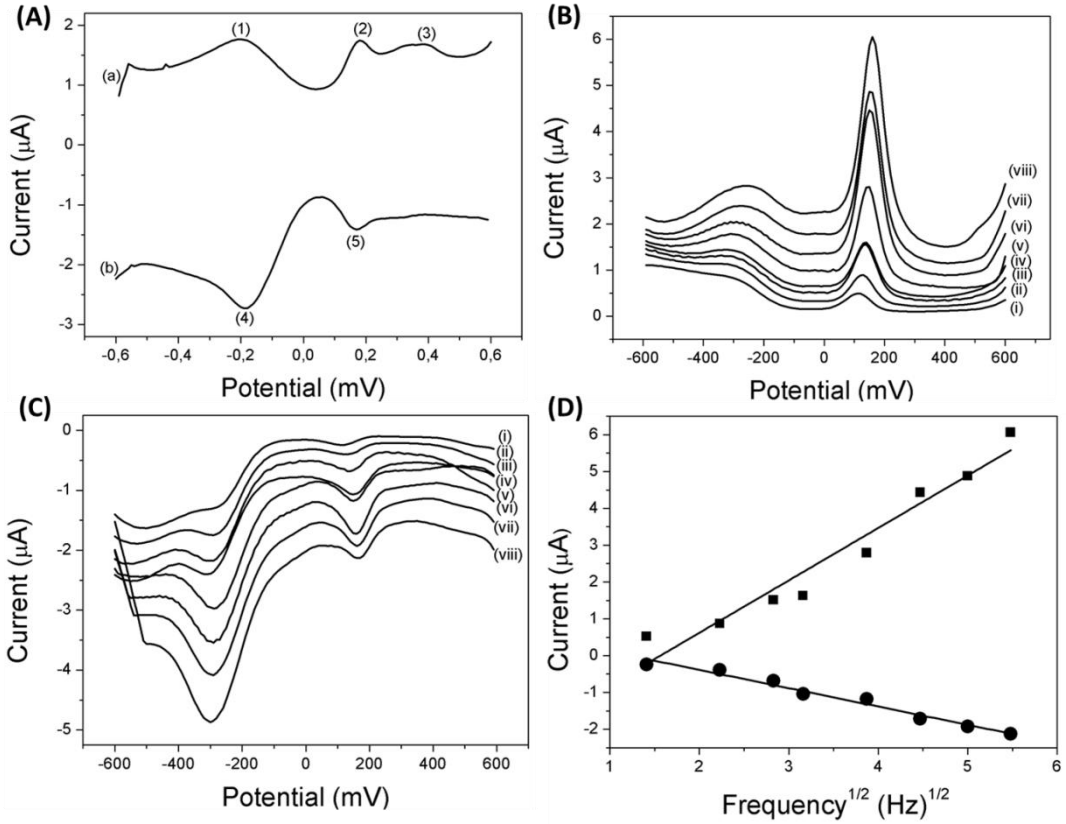


**Figure 8**. (A) square wave voltammograms of (a) anodic and (b) cathodic scans of CuPPI coated gold electrode at 10 Hz (B) anodic square wave voltammogram of PPI coated gold electrode at frequencies of (i) 2 (ii) 5 (iii) 8 (iv) 10 (v) 15 (vi) 20 (vii) 25 and (viii) 30 Hz (C) cathodic square wave voltammograms of PPI coated gold electrode at above frequencies (D) linear plot of current vs frequency. All of the above were carried out under aerobic conditions.

## 4. CONCLUSION

In this work a poly(propyleneimine) based dendrimer was characterised along with its copper functionalised counterpart. Both compounds were studies using fourier transform infrared spectroscopy (FTIR), atomic force microscopy (AFM), high resolution transmission electron

microscopy (HR-TEM) as well as high resolution scanning electron microscopy (HR-SEM). Differences in the structure of the two dendrimers were found and attributed to the presence of copper which made the compound crystalline. The dendrimers were also characterised using voltammetric techniques and both were found to be electroactive, with the copper metallodendrimer proving to be a more viable candidate for electrocatalytic purposes. When comparing the performance of the metallodendrimer in anaerobic and aerobic conditions we can see the difference between the two systems. It is clear that the presence of oxygen affects the characteristics of the CuPPI metallodendrimer. In this case it slightly diminishes the current flow in the system since it is clear that the peaks attributed to the CuPPI action decrease in current intensity in both the anodic and cathodic sweeps of the CV. In this case the diffusion coefficient also slightly decreases from $4.124 \times 10^{-5}$ $cm^2$ $s^{-1}$ in the absence of oxygen to $3.29 \times 10^{-5}$ $cm^2$ $s^{-1}$ when oxygen was present. The copper metallodendrimer has proven to have favorable characteristics for application as an electrocatalytic platform for electrochemical biosensors.

ACKNOWLEDGEMENTS
This study was funded by the National Research Foundation of South Africa. We would also like to acknowledge Sensorlab Research Group and the Chemistry department at the University of the Western Cape.

## References

1. E. Frechet and J. Gillies., *Drug Discovery Today*, 10 (2005) 35.
2. J. Reek, D. deGroot, G. Oosterom, P. Kamer and P. vanLeeuwen, *Rev. Mol. Biotechnol.*, 90 (2002) 159.
3. M. Venturi, S. Serroni, A. Juris, S. Campagna and V. Balzani, *Dendrimers*, Springer Berlin Heidelberg, Berlin (1998) 193.
4. C. Nijhuis, B. A. Noukamp, B. J. Ravoo, J. Huskens and D. N. Reinhoudt, *J. Phys. Chem. C*, 111 (2007) 9799.
5. P. Kersharwani, K. Jain and N. Jain, *Prog. Polym., Sci*. 39 (2014) 268.
6. C. Braun, J. Vetro, D. Tomalia, G. Koe, J. Koe and C. Middaugh, *J. Pharm. Sci*., 94 (2005) 423.
7. E. Wiener, M. Brechbiel, H. Brothers, R. Magin, O. Gansow, D. Tomalia and P. Lauterbur, *Magn. Reson. Med.*, 31 (1994) 1.
8. A. Bosnjakovic, M. Mishra, H. Han, R. Romero and R. Kannan, *Anal. Chim. Acta*, 720 (2012) 118.
9. O. Finikova, A. Galkin, V. Rozhkov, M. Cordero, C. Hagerhall and S. Vinogradov, *J. Am. Chem. Soc*, 125 (2003) 4882.
10. Z. Li and J. Li, *Curr. Org. Chem*., 17 (2013) 1334.
11. D. Mery and D. Astruc, *Coord. Chem. Rev*, 250 (2006) 1965.
12. N. Krasteva, B. Guse, I. Besnard, A. Yasuda and T. Vossmeyer, *Sens. Actuators, B*, 92 (2003) 137.
13. A. Grabchev, S. Dumas and J. Chovelon, *Dyes Pigments*, 82 (2009) 36.
14. J. Martinovic, J. v. Wyk, S. Mapolie, N. Jahed, P. Baker and E. Iwuoha, *Electrochim. Acta*, 55 (2010) 4296.
15. A. Chen and S. Chatterjee, *Chem. Soc. Rev.*, 42 (2013) 5425.
16. J. Martinovic, A. Chiorcea-Parquim, V. Diculescu, J. v. Wyk, E. Iwuoha, S. Mapolie and A. Oliveira-Brett, *Electrochim. Acta*, 53 (2008) 4907.
17. J. Mugo, S. Mapolie and J. vanWyk, *Inorg. Chim. Acta.*, 363 (2010) 2643.

18. J. vanWyk, S. mapolie, A. Lennartson, M. Hakansson and S. Jagner, *Inorg. Chim. Acta.*, 361 (2008) 2094.
19. V. Vellora, T. Padil and M. Cernik, *Int. J. Nanomedicine.*,8 (2013) 889.
20. P. L. Hansen, J. B. Wagner, S. Helveg, J. R. Rostrup-Nielsen, B. S. Clausen and H. Topsee, *Science*, 295 (2002) 2053.
21. A. J. Bard and L. R. Faulkner, *Electrochemical Methods: Fundamentals and Applications*, John Wiley & Sons, New York (1980).
22. A. J. Bard and L. R. Faulkner, *Electrochemical Methods: Fundamentals and Applications*, 2 ed., John Wiley & Sons New York (2001).
23. A. P. Brown and F. C. Anson, *Anal. Chem.*, 49 (1977) 1589.
24. J. E. B. Randles, *J. Chem. Soc. Faraday Trans.*, vol. 48, pp. 828-832, 1952.